Tuning Adsorption Energies and Reaction Pathways by Alloying: PdZn versus Pd for CO2 Hydrogenation to Methanol

F. Brix, V. Desbuis, L. Piccolo, E. Gaudry

Tuning adsorption energies and reaction pathways by alloying : PdZn versus Pd for CO_2 reduction to methanol

Florian Brix[1], Valentin Desbuis[1,2], Laurent Piccolo[3], Émilie Gaudry[1,2*]

[1] *Univ. Lorraine, CNRS, Institut Jean Lamour, Campus Artem, 2 Allée André Guinier, F-54011, Nancy, France*
[2] *École des Mines de Nancy, Campus Artem, CS 14 234, 92 Rue Sergent Blandan, 54042 Nancy, France*
[3] *Univ Lyon, Université Claude Bernard Lyon 1, CNRS, IRCELYON, F-69626, Villeurbanne, France*

E-mail: emilie.gaudry@univ-lorraine.fr

Abstract

The tunability offered by alloying different elements is useful to design catalysts with greater activity, selectivity, and stability than single metals. By comparing the Pd(111) and PdZn(111) model catalysts for CO_2 hydrogenation to methanol, we show that intermetallic alloying is a possible strategy to control the reaction pathway from the tuning of adsorbate binding energies. In comparison to Pd, the strong electron-donor character of PdZn weakens the adsorption of carbon-bound species and strengthens the binding of oxygen-bound species. As a consequence, the first step of CO_2 hydrogenation more likely leads to the formate intermediate on PdZn, while the carboxyl intermediate is preferentially formed on Pd. This results in the opening of a pathway from carbon dioxide to methanol on PdZn similar to that previously proposed on Cu. These findings rationalize the superiority of PdZn over Pd for CO_2 conversion into methanol, and suggest guidance for designing more efficient catalysts by promoting the proper reaction intermediates.

The reduction of CO_2 greenhouse gas emissions and the availability of a reliable, and secure carbon-neutral energy supply are vital in order to slow down the rate of climate change while replacing fossil sources.[1] Anthropogenic CO_2 conversion to methanol can help to face this double challenge.[2,3] Methanol is a safe, easily transportable and fastly biodegradable liquid fuel which can be used with today's vehicle technology at minimal incremental costs.[4] Catalytic CO_2 hydrogenation to methanol (CO_2+H_2→H_2O+H_3COH), with hydrogen produced from water electrolysis, has proven to be a viable process at the pilot plant scale in several countries.[5] Because CO_2 is a very stable molecule, highly efficient catalysts are required to reduce it to methanol. For now, the Cu-ZnO-Al_2O_3 catalyst, initially developed for CO hydrogenation to methanol, is used in combination with harsh pressure conditions (> 50 bar).[6] In this context, the design of more efficient catalysts for decreasing the pressure as well as the temperature is an active field of research. Two main strategies are currently used to design new catalysts for CO_2 hydrogenation to methanol. First, the conception of copper-metal oxide interfaces such as Cu/ZnO, Cu/CeO_2, and Cu/ZrO_2[7–10] has been reported to promote the formation of formate, thus increasing catalytic activity and selectivity[11] Another decisive approach is based on engineering the coordination environment of active metal atoms by alloying,[12,13] to control the reaction pathways that drive the chemical transformations. For instance, alloying Ni with Ga penalizes the rWGS (reverse Water Gas Shift) reaction on NiGa catalysts, thereby facilitating the production of methanol.[14]

Several Pd-based compounds are recognized as attractive catalysts for CO_2 reduction to methanol. Compared to Cu-based catalysts, they can be chemically stable, resistant to sintering,[15–17] and present superior activity toward methanol production at lower temperatures.[18–20] Current interest in this direction has been focused on several systems, such as Pd/ZnO,[21,22] Pd/Ga_2O_3,[23,24] Pd/In_2O_3[23,25] or Pd/ZrO_2.[26] The performances of Pd/ZnO are generally ascribed to the formation of the PdZn intermetallic compound at the oxide surface by reduction of the powder catalyst under H_2 at high temperature ($T > 200^oC$).[27–30] The formation of heteroatomic bonds in PdZn, driven by electron transfer from Zn to Pd ($Zn^{0.4+}Pd^{0.4-}$),[31] changes the electronic environment of the active metal. Focusing on methanol steam reforming (MSR), which is the reverse reaction of methanol synthesis from CO_2 and H_2, a clear correlation between electronic structure and CO_2 selectivity was recently obtained by comparing Cu with PdZn, PtZn, NiZn, and PdCd intermetallics on the basis of experiments and calculations.[32] The specific electronic structure of PdZn, characterized by a shift towards higher binding energies of the Pd *d*-band upon alloying, makes the density of states of the alloy resemble that of Cu.[33] This accounts for the similar catalytic performances of the two catalysts.[32] At the atomic scale, a correlation between adsorption energies and CO_2 selectivity pointed the key role of formaldehyde, a weak adsorption of H_2CO leading to a high theoretical selectivity.[34] Experimentally, the addition of Pd to ZnO was shown to slightly lower the thermodynamic stability of adsorbed formaldehyde, which correlates with increased selectivities to CO_2 and H_2.[35] Meanwhile, the high activity was attributed to identical adsorption energies of methanol and water on PdZn/ZnO – as determined from micro-calorimetry and infrared spectroscopy, since methanol could competitively adsorb and react with water. However, no extensive mechanistic studies have been performed so far to relate the reaction paths of CO_2 hydrogenation to methanol on the PdZn catalysts, and thereby clearly reveal the role of alloying Pd with Zn.[35] Herein, using plane-wave density functional theory (DFT) calculations, we investigate how the addition of an ancillary metal (Zn) to a metallic catalyst (Pd) influences the mechanism of methanol synthesis through CO_2 hydrogenation. The theoretical study has been performed at P=0 and T=0. It is a mandatory first step towards the investigation and in-depth understanding of the alloying effect on the catalytic performances. We chose the Pd(111) and PdZn(111) surfaces, because this orientation is the most stable for both systems[36–38] and has been observed experimentally.[39] Adsorption (E_{ads}) and reaction (ΔE) energies were systematically determined based on total energy calculations (section S1, Tabs S1-S5, Figs. S1-S5), while activation energies (E_{act}) were ruled on by the climbing image nudged elastic band (CI-NEB) method (Fig. S6, Tab. S5).[40–43]

On both catalysts, carbon dioxide does not form stable chemical adsorption state (Fig. S2), similarly to what happens on other dense metallic surfaces,[44] where CO_2 is weakly physisorbed or unstable.[45] After the structural optimization, the molecule stands parallel and rather far from the surface (distance larger than 3 Å). No activation of CO_2 is identified at this stage: adsorption strengths are weak – but almost twice larger on PdZn than on Pd (Fig. S2) – and the C-O bond lengths computed for CO_2 physisorbed on Pd and PdZn are equal to the ones calculated for the gas phase (1.18 Å).

Considering all other species involved in CO_2 hydrogenation to methanol, alloying Pd with Zn leads to drastic modifications of the catalyst adsorption properties (Fig. 1). The adsorption energies of carbon-bound species – CO, HCO, H_2CO, COOH, COH, HCOH, $C(OH)_2$, H_2COH – are strengthened on Pd, the largest changes being calculated for H_2CO, COH, $C(OH)_2$. In contrast, oxygen-bound species – H_3COH, O, HO, H_2O, H_3CO, HCOOH, HCOO, H_2COOH, H_2COO – interact more strongly with PdZn(111), especially H_2O. In regard to charge transfer, which is a key parameter for adsorption properties, this behavior can been attributed to the substantial electron-donating and weak electron-accepting ability of PdZn, resulting from its fully filled d-states.[46] In comparison, Pd presents an

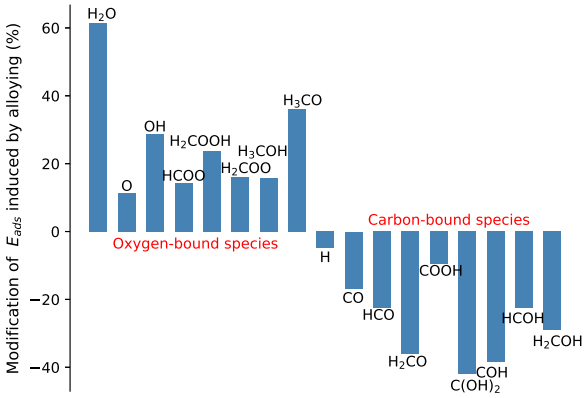

Figure 1: Modification of the catalyst adsorption properties due to alloying Pd with Zn. The relative changes are evaluated by $(E_{ads}^{PdZn} - E_{ads}^{Pd})/E_{ads}^{Pd}$, using data from Tabs S1-S4. A positive (resp. negative) value means that the adsorbate is more (resp. less) strongly adsorbed on PdZn than on Pd. The adsorption energies of the HCOOH intermediate are identical on PdZn and Pd.

electron-accepting and a weak electron-donating character, due to its partially filled d-states. Such an electronic effect also explains the larger modification of the water adsorption energy, induced by alloying, than of the methanol one, both adsorbed at top sites – top-Zn or top-Pd site on PdZn and Pd, respectively – since the oxygen electronegativity in methanol is weaker than in water (14.87 eV.e^{-1} and 19.79 eV.e^{-1}, respectively).[47] Alloying can change the binding mode of the adsorbates as well. For example, H_3CO bounds to the surface through the oxygen atom, at a hollow site on Pd but at a bridge site on PdZn, thus maximizing O-Zn interactions on PdZn. A similar behavior can be observed for carbon-bound adsorbates, such as H, CO and COH, located in a hollow site on Pd and in a bridge Pd-Pd site on PdZn, which is likely to maximize the C-Pd interactions. The larger Pd-Pd distance at the PdZn(111) surface (4.41 Å) than at the Pd(111) surface (2.75 Å) may also contribute to the change of the binding mode, as observed for HCOH and c-COOH (*cis*-COOH), lying at top-Pd and bridge sites on PdZn and Pd, respectively.

So far, theoretical studies have identified three main reaction routes for methanol synthesis from CO_2[48] (Fig. 2, black arrows). The conventionally proposed pathways are the *formate pathways*, during which CO_2 is first hydrogenated to formate (HCOO), the latter being hydrogenated to H_2CO through H_2COO or HCOOH followed by H_2COOH, and then methanol. This mechanism has been frequently invoked for Cu surfaces,[49–52] as well as for several Cu/oxide,[53–57] Cu/carbide,[58] Cu alloys,[59–61] and Pd/oxide[62,63] catalysts. Alternatively, the *CO pathway* is generally assumed to explain the formation of the CO byproduct, as observed for some Cu/oxide,[7,10] doped-Cu catalysts[64] or Cu-based alloys.[65] The formation of CO results from CO_2 hydrogenation via the COOH intermediate, and methanol is produced from CO hydrogenation through HCO and H_2CO. For Pd, our results point towards this mechanism as well (Fig. 2, blue arrows). The first hydrogenation step to c-COOH occurs with a rather large barrier (Figs 3, S6 and Tab. S5), while carbon monoxide forms from c-COOH rather easily (E_{act}^{Pd}(c-COOH → CO) = 0.59 eV), compared to the one leading to HCOOH (E_{act}^{Pd}(c-COOH → HCOOH) = 1.01 eV). This is in agreement with the substantial CO selectivity from CO_2 hydrogenation over Pd black, as experimentally measured.[25] Methanol is then obtained from CO, through HCO, H_2CO, H_2COH species (Figs. 3, S6 and Tab. S5), which have all been experimentally observed upon methanol decomposition on Pd.[66] However, several elementary steps present rather large activation energies: CO → HCO (E_{act}^{Pd} = 1.09 eV), HCO → H_2CO (E_{act}^{Pd} = 0.97 eV), and H_2CO → H_2COH (E_{act}^{Pd} = 0.70 eV). This may explain why methanol is not produced from CO_2 or CO hydrogenation on Pd.[25] The *COOH pathway* is less frequently adopted in the literature.[44,48,67] A few examples include the catalysis by intermetallic compounds (Ga_3Ni_5,[68] $PdCu_3$[69]) and oxidized copper, surface oxygen or water-derived species facilitating the formation of methanol.[70]

On PdZn, like on Pd, the spontaneous dissociate adsorption of H_2 can provide enough H coverage and promote subsequent reactions (Tab. S5). In addition, like on Pd, direct formation of CO from CO_2 is not likely on PdZn, since it proceeds through large barriers on both catalysts ($E_{act} > 1.5$ eV, Tab. S5). The crucial step to determine the reaction pathway is the first elementary step of CO_2 hydrogenation, which consists in formate (HCOO) or carboxyl (COOH) formation. As shown in Fig. 1, alloying Pd with Zn results in a slight stabilization (relative change of the adsorption energy by -14%) of the formate species at the alloy surface and in a faint destabilization of the carboxyl species (+10%). Thus, the *formate pathways* are expected to be more favorable on PdZn. The previous picture is validated by NEB calculations, as explained in the following (Fig. 2, red arrows).

The formation of HCOO from CO_2 is found slightly exothermic (Tab. S5), with a smaller barrier on PdZn than on Cu(111) (E_{act}^{PdZn}=0.58 eV; $E_{act}^{Cu(111)}$ = 0.87 eV[52]). These findings are consistent with the presence of formate species on the PdZn surface, as experimentally observed[21,71] Alloying is thus demonstrated to change the picture, the formation of HCOO from CO_2 being endothermic on Pd, and occurring with a huge barrier (E_{act}^{Pd} = 2.23 eV). No activation of the CO_2 molecule is compulsory on PdZn, in contrast to what has been proposed by Zhang *et al.* on Pd, starting from activated CO_2, adsorbed in a bidendate configuration ($E_{ads}^{Pd} > 0$) to make the *formate pathway* achievable. Comparable trends have been calculated by alloying Pd with other metals, whether the considered active surface presents a similar surface structure ($E_{act}^{PdIn(110)}$ = 0.05 eV)[72] or not ($E_{act}^{PdCu(111)}$ = 0.62 eV).[73] Once HCOO is

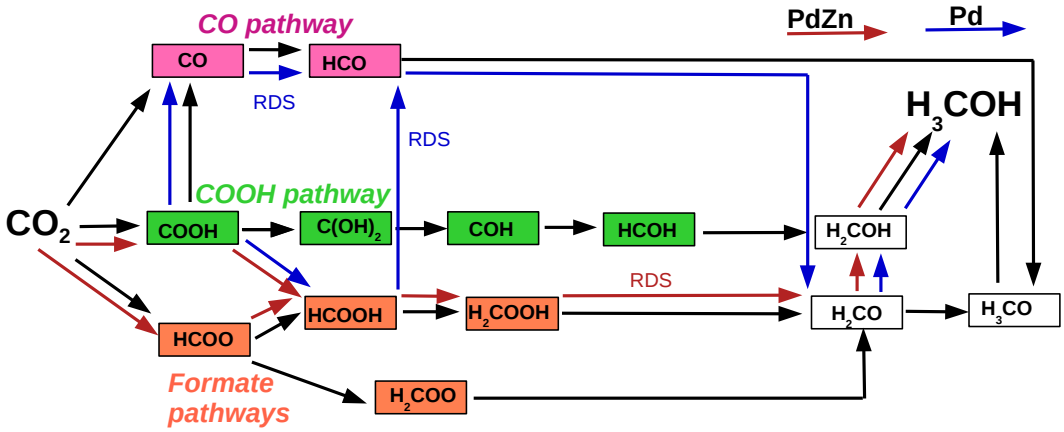

Figure 2: Main reaction routes frequently reported in literature, for methanol synthesis from CO_2 hydrogenation (black arrows). The most energetically favorable pathways identified herein for Pd and PdZn are shown with blue and red arrows, respectively. The rate-determining steps on Pd and PdZn, identified from Tab. S5 and Fig. S6, are labeled "RDS".

formed, several steps can be considered (Fig. S6, Tab. S5). Breaking the C-O bond to form HCO+OH is not likely (E_{act}^{PdZn} = 2.33 eV). Similarly, H_2COO proceeds through a large barrier (E_{act}^{PdZn} = 1.56 eV). In contrast, the hydrogenation of HCOO to formic acid (HCOOH) is probable (Fig. 3), with an activation energy smaller than on Pd (E_{act}^{Pd} = 0.73 eV; E_{act}^{PdZn} = 0.52 eV) and Cu(111) ($E_{act}^{Cu(111)}$ = 0.91 eV[52]). The modification of the activation energy is found to strongly depend on the ancillary metal with which Pd is combined : $E_{act}^{PdIn(110)}$ = 0.65 eV[72] and $E_{act}^{PdCu(111)}$ = 1.28 eV.[73] The scenario on PdZn(111) differs from studies on Cu(111) in which H_2COO has been frequently invoked as the product of HCOO hydrogenation.[52] Formaldehyde, that is more stabilized on Pd than PdZn, likewise results from the C-O bond breaking in H_2COOH, which is more stabilized on PdZn than on Pd (Fig. 1). Thus, the reaction is not thermodynamically favored on PdZn (ΔE^{PdZn} = 0.59 eV, Tab. S5) and the barrier is the rate determining step (E_{act}^{PdZn} = 0.90 eV, Fig. 3).

As shown before, alloying stabilizes the formate species at the PdZn surface, thus facilitating the *formate pathways*, and destabilizes the carboxyl species. However, the latter effect is small (10% increase in adsorption energy, in average). Is it enough to avoid the formation of the carboxyl species at the PdZn alloy surface? On PdZn, CO_2 hydrogenation to COOH is found competitive with the formation of HCOO (Fig. 3). The reaction is endothermic for both the *cis* and *trans* COOH isomers (Tab. S5). The activation energies to form t-COOH and HCOO are almost the same and moderate ($E_{act}^{PdZn}(CO_2 \rightarrow$ t-COOH) = 0.61 eV and $E_{act}^{PdZn}(CO_2 \rightarrow$ HCOO) = 0.58 eV). On PdZn, the c-COOH configuration – less adsorbed on PdZn than Pd (Fig. 1) and resulting from isomerization (E_{act}^{PdZn}(t-COOH $\rightarrow$ c-COOH) = 0.66 eV) – provides an optimized geometry to spontaneously convert into formic acid, an intermediate more strongly adsorbed on PdZn than on Pd (E_{act}^{PdZn}(c-COOH$\rightarrow$ HCOOH) = 0.03 eV). The latter can then react according to the *formate mechanism* detailed before. Such a step has not been invoked so frequently in literature for CO_2 reduction to methanol, the corresponding barriers being usually much larger ($E_{act}^{Ga_3Ni_5(221)}$ = 0.93 eV,[68] $E_{act}^{Cu(111)}$ = 0.64 eV,[74] $E_{act}^{Pd(111)}$ = 0.75 eV[75]). The previous scenario, as an hybrid pathway between the formate and COOH ones (Fig. 3), is more likely than the one following the complete *COOH mechanism*. Indeed, the hydrogenation of COOH to $C(OH)_2$ is endothermic and occurs with rather large barriers (ΔE^{PdZn} = 1.01 eV, E_{act}^{PdZn} = 1.02 eV).

As demonstrated in the previous sections, formaldehyde is a key intermediate in the CO_2 hydrogenation to methanol. This carbon-bound species is more strongly adsorbed on Pd than on PdZn (Fig. 1, Tab. S2), in agreement with other theoretical calculations.[76] This tendency is however reverse to the experimental findings, suggesting that formaldehyde is more strongly bound on PdZn.[77,78] This may arise from the structural complexity of actual catalyst surfaces, as well as the influence of reaction conditions. The addition of Zn changes the most favorable adsorption site from $\eta^1_{Pd}(C)\eta^1_{Pd}(O)$ on Pd (Fig. S5) to $\eta^1_{Pd}(C)\eta^3_{PdZn_2}(O)$ on PdZn (Fig. S4), in agreement with the results of Smith *et al.*[79] The experimental observations by Jeroro and Vohs, who reported that H_2CO binds to Pd-Zn dimers, with the carbon end of the molecule bound to Pd and the oxygen end bound to Zn,[77] slightly differ from our findings. Starting from formaldehyde, the methanol formation can proceed through H_3CO or H_2COH (Fig. 3). The barriers are smaller through H_2COH than through H_3CO (Tab. S5), which is attributed to the specific configuration of adsorbed H_2COH, with the C-O bond almost parallel to the surface (Figs. S4-S5). Alloying Pd with Zn again facilitates the transformation from H_2CO to methanol, the barriers being smaller on PdZn than

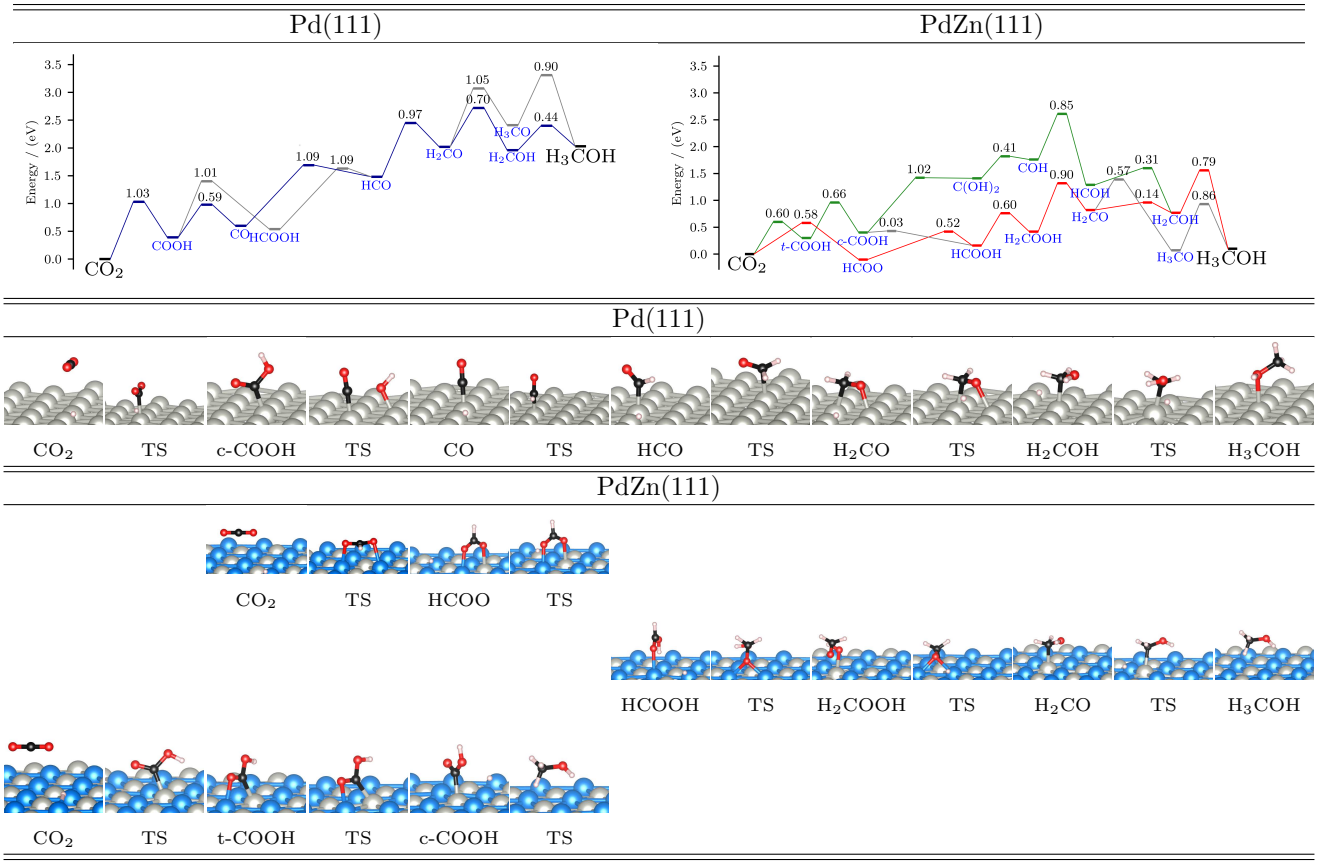

Figure 3: Top : Energy landscape for CO_2 hydrogenation to methanol on Pd and PdZn. The values indicated on the graph represent the activation energy barriers in eV. *Formate, COOH and CO pathways* are depicted in red, green and blue, respectively. Alternative paths are shown in gray. Bottom : Adsorbates and transition states (TS) structures. c-COOH and t-COOH stands for *cis*-COOH and *trans*-COOH, respectively.

on Pd (Fig. S6, Tab. S5). This last sequence is quite different to what is generally proposed in the literature, i.e. the hydrogenation of H_2CO to H_3CO and methanol, as found by Zhang et al. on Pd(111),[80] Wu and Yang on PdIn(110),[72] and Nie *et al.* on PdCu(111).[73]

In summary, alloying Pd with Zn strongly alters the preferred binding configuration of several intermediates, such as CO, H_2CO and H_3CO. This deeply modifies the kinetically preferred pathway to methanol. The latter more likely proceeds through the *formate* mechanism, thus avoiding the formation of CO, in agreement with the experimental observations.[21,25] Such a reaction path is very similar to the one calculated on Cu(111)[52] – $CO_2 \rightarrow HCOO \rightarrow HCOOH \rightarrow H_2COOH \rightarrow H_2CO \rightarrow H_2COH \rightarrow H_3COH$. On both PdZn and Cu, the steps with the highest barriers are the C-O bond breaking to formaldehyde and H addition to H_2COH (Fig. 3, Tab. S5). Overall, barriers are lower on PdZn than on Pd, in agreement with the superior methanol yields measured for catalysts containing the PdZn intermetallic phase.[25,81] The insights gained by studying the reaction networks on PdZn versus Pd shed light on its intrinsic catalytic properties at T=0 and P=0. Further work will include other effects such as the influence of the support and the reaction conditions on the catalytic properties. The extension of our study to other ancillary metals combined with Pd may stimulate the discovery of novel alloy catalysts for CO_2 hydrogenation to alcohols.

Computational methods

All calculations were performed based on the Density Functional Theory (DFT) using the Vienna *ab initio* simulation package (VASP).[82–84] The interaction between the valence electrons and the ionic core was described using the spin polarized projector-augmented wave (PAW) method[85,86] within the generalized gradient approximation of Perdew, Burke and Ernzerhof (GGA-PBE),[87] considering the valences for the atoms to be $4d^9 5s^1$ (Pd), $4d^{10}p^2$ (Zn), $2s^2 2p^4$ (O) $2s^2 2p^2$ (C) and $1s^1$ (H). To compensate for a poor description of van der Waals interactions by GGA functionals, the D3 correction method by Grimme was employed.[88] Structures were relaxed until the forces dropped below 0.01 eV/Å. Reaction energies (ΔE) were determined, as well as energy barriers (E_{act}), based on the climbing image nudged elastic band (CI-NEB) method.[40–43] Seven intermediate images were produced by linear interpolations between relaxed images. The optimization was stopped when the change in the total (free) energy was smaller than 10^{-4} eV. Vibrational analysis (for saddle

point verification), limited to the surface species and keeping the rest of the system fixed, was carried out by calculating Hessian matrix with finite difference approach with a step size of 0.015 Å.

One-electron Kohn-Sham orbitals were expanded with a kinetic energy cutoff of 450 eV. The reciprocal space integration was approximated with a Monkhorst-Pack k-point grid of 9×9×9, 2×4×1 and 3×3×1 for the bulk crystals, PdZn(111) and Pd(111) catalytic surfaces, respectively. This setup leads to lattice parameters for the PdZn (P4/mmm space group, a = 4.12 Å, c = 3.42 Å), in good agreement with other theoretical values (a = 4.14 Å, c = 3.38 Å;[89] a = 4.15 Å, c = 3.39 Å[39]), as well as with experimental ones (interpolated values for 50 at. % Zn, a= 4.11 Å and c = 3.35 Å[39,90]). All calculations have been performed using a bulk truncated model, since the strength of Pd-Zn bonds was demonstrated to prevent any surface segregation in the self-supported 1:1 alloy film.[39]

Associated content

Summary of adsorption properties of Pd(111) and PdZn(111) towards all intermediates involved in the CO_2 reduction to methanol (adsorption energies and configurations); Scheme of all considered reaction paths; Table containing the corresponding reaction and activation energies.

Acknowledgment

This work is supported by the European Integrated Center for the Development of New Metallic Alloys and Compounds. We acknowledge financial support through the COMETE project (COnception in silico de Matériaux pour l'EnvironnemenT et l'Énergie) cofunded by the European Union under the program *F*EDER-FSE Lorraine et Massif des Vosges 2014-2020. This work was granted access to the HPC resources of TGCC, CINES and IDRIS under the allocation 99642 attributed by GENCI (Grand Equipement National de Calcul Intensif). High Performance Computing resources were also partially provided by the EXPLOR centre hosted by the University de Lorraine (project 2017M4XXX0108).

The authors declare no competing financial interest

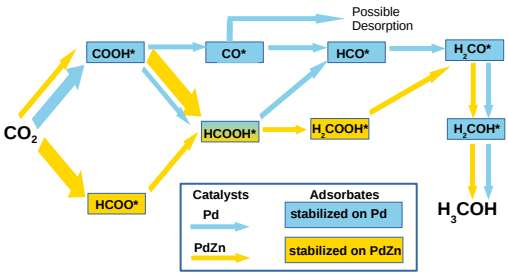
Possible
Desorption
COOH*
CO*
HCO*
H2CO*
CO2
HCOOH*
H2COOH*
H2COH*
HCOO*
H3COH
Catalysts
Adsorbates
Pd
stabilized on Pd
PdZn
stabilized on PdZn

References

(1) Cozzi, L.; Gould, T. *World Energy Outlook*; 2019.

(2) Olah, G. A. Beyond oil and gas: the methanol economy. *Angew. Chem. Int. Ed.* **2005**, *44*, 2636–2639.

(3) Palo, D. R.; Dagle, R. A.; Holladay, J. D. Methanol steam reforming for hydrogen production. *Chemical reviews* **2007**, *107*, 3992–4021.

(4) Trimm, D. L.; Önsan, Z. I. Onboard fuel conversion for hydrogen-fuel-cell-driven vehicles. *Catalysis Reviews* **2001**, *43*, 31–84.

(5) Atsonios, K.; Panopoulos, K.; Kakaras, E. Investigation of technical and economic aspects for methanol production through CO_2 hydrogenation. *International Journal of Hydrogen Energy* **2015**, *41*, 2202–2214.

(6) Waugh, K. Methanol synthesis. *Catal. Today* **1992**, *15*, 51–75.

(7) Kattel, S.; Liu, P.; Chen, J. G. Tuning Selectivity of CO_2 Hydrogenation Reactions at the Metal/Oxide Interface. *J. Am. Chem. Soc.* **2017**, *139*, 9739–9754.

(8) Liao, F.; Zeng, Z.; Eley, C.; Hong, Q. L. X.; Tsang, S. Electronic Modulation of a Copper/Zinc Oxide Catalyst by a Heterojunction for Selective Hydrogenation of Carbon Dioxide to Methanol. *Angew. Chem. Int. Ed.* **2012**, *51*, 5832–5836.

(9) Liu, C.; Yang, B.; Tyo, E.; Seifert, S.; DeBartolo, J.; von Issendorff, B.; Zapol, P.; Vajda, S.; Curtiss, L. A. Carbon Dioxide Conversion to Methanol over Size-Selected Cu4 Clusters at Low Pressures. *J. Am. Chem. Soc.* **2015**, *137*, 8676–8679.

(10) Graciani, J.; Mudiyanselage, K.; Xu, F.; Baber, A. E.; Evans, J.; Senanayake, S. D.; Stacchiola, D. J.; Liu, P.; Hrbek, J.; Fernandez-Sanz, J. et al. Highly active copper-ceria and copper-ceria-titania catalysts for methanol synthesis from CO_2. *Science* **2014**, *345*, 546–550.

(11) Chen, Y.; Li, H.; Zhao, W.; Zhang, W.; Li, J.; Li, W.; Zheng, X.; Yan, W.; Zhang, W.; Zhu, J. et al. Optimizing Reaction Paths for Methanol Synthesis from CO_2 Hydrogenation via Metal-Ligand Cooperativity. *Nat. Commun.* **2019**, *10*, 1885.

(12) van-den Berg, R.; Prieto, G.; Korpershoek, G.; van-der Wal, L. I.; van Bunningen, A. J.; Laegsgaard-Jorgensen, S.; de Jongh, P. E.; de Jong, K. P. Structure sensitivity of Cu and CuZn catalysts relevant to industrial methanol synthesis. *Nat. Comm.* **2016**, *7*, 13057.

(13) Khan, M. U.; Wang, L.; Liu, Z.; Gao, Z.; Wang, S.; Li, H.; Zhang, W.; Wang, M.; Wang, Z.; Ma, C. et al. Pt_3Co Octapods as Superior Catalysts of CO_2 Hydrogenation. *Angew. Chem. Int. Ed.* **2016**, *55*, 9548.

(14) Studt, F.; Sharafutdinov, I.; Abild-Pedersen, F.; Elkjaer, C.; Hummelshoj, J.; Dahl, S.; Chorkendorff, I.; Norskov, J. Discovery of a Ni-Ga catalyst for carbon dioxide reduction to methanol. *Nat. Chem.* **2014**, *6*, 320–324.

(15) Ma, J.; Sun, N.; Zhang, X.; Zhao, N.; Xiao, F.; Wei, W.; Sun, Y. A short review of catalysis for CO_2 conversion. *Catal. Today* **2009**, *148*, 221–231.

(16) Shen, W.; Ichihashi, Y.; Ando, H.; Matsumura, Y.; Okumura, M.; Haruta, M. Influence of Palladium Precursors On Methanol Synthesis From CO Hydrogenation over Pd/CeO_2 Catalysts Prepared by Deposition–Precipitation Method. *Appl. Catal. A* **2001**, *217*, 165–172.

(17) Conant, T.; Karim, A. M.; Lebarbier, V.; Wang, Y.; Girgsdies, F.; Schlögl, R.; Datye, A. Stability of bimetallic Pd-Zn catalysts for the steam reforming of methanol. *Journal of Catalysis* **2008**, *257*, 64–70.

(18) Poutsma, M. L.; Elek, L. F.; Ibarbia, P. A.; Risch, A. P.; Rabo, J. Selective Formation of Methanol from Synthesis Gas over Palladium Catalysts. *J. Catal.* **1978**, *52*, 157–168.

(19) Gotti, A.; Prins, R. Basic Metal Oxides as Co-catalysts in the Conversion of Synthesis Gas to Methanol on Supported Palladium Catalysts. *J. Catal.* **1998**, *175*, 302–311.

(20) Matsumura, Y.; Shen, W. J.; Ichihashi, Y.; Okumura, M. Low Temperature Methanol Synthesis Catalyzed over Ultrafine Palladium Particles Supported on Cerium Oxide. *J. Catal.* **2001**, *197*, 267–272.

(21) Bahruji, H.; Bowker, M.; Hutchings, G.; Dimitratos, N.; Wells, P.; Gibson, E.; Jones, W.; Brookes, C.; Morgan, D.; Lalev, G. Pd/ZnO catalysts for direct CO_2 hydrogenation to methanol. *J. Catal.* **2016**, *343*, 133–146.

(22) Iwasa, N.; Kudo, S.; Takahashi, H.; Masuda, S.; Takezawa, N. Highly selective supported Pd catalysts for steam reforming of methanol. *Catalysis Letters* **1993**, *19*, 211–216.

(23) Collins, S. E.; Delgado, J. J.; Mira, C.; Calvino, J. J.; Bernal, S.; Chiavassa, D. L.; Baltanás, M. A.; Bonivardi, A. L. The role of Pd-Ga bimetallic particles in the bifunctional mechanism of selective methanol synthesis via CO_2 hydrogenation on a Pd/Ga_2O_3 catalyst. *J. Catal.* **2012**, *292*, 90–98.

(24) Rui, N.; Wang, Z.; Sun, K.; Ye, J.; Ge, Q.; Liu, C.-J. CO_2 hydrogenation to methanol over Pd/In_2O_3: effects of Pd and oxygen vacancy. *Applied Catalysis B: Environmental* **2017**, *218*, 488–497.

(25) Iwasa, N.; Suzuki, H.; Terashita, M.; Arai, M.; Takezawa, N. Methanol synthesis from CO_2 under atmospheric pressure over supported Pd catalysts. *Catalysis letters* **2004**, *96*, 75–78.

(26) Fujitani, T.; Nakamura, I. Methanol synthesis from CO and CO_2 hydrogenations over supported palladium catalysts. *Bull. Chem. Soc. Jpn.* **2002**, *75*, 1393–1398.

(27) Tew, M.; Emerich, H.; van Bokhoven, J. Formation and Characterization of PdZn Alloy: A Very Selective Catalyst for Alkyne Semihydrogenation. *J. Phys. Chem. C* **2011**, *115*, 8457–8465.

(28) Niu, Y.; Liu, X.; Wang, Y.; Zhou, S.; Lv, Z.; Zhang, L.; Shi, W.; Li, Y.; Zhang, W.; Su, D. et al. Visualizing Formation of Intermetallic PdZn in a Palladium/Zinc Oxide Catalyst: Interfacial Fertilization by PdH_x. *Angewandte Chemie International Edition* **2019**, *58*, 4232–4237.

(29) Xu, J.; Su, X.; Liu, X.; Pan, X.; Pei, G.; Huang, Y.; Wang, X.; Zhang, T.; Geng, H. Methanol synthesis from CO_2 and H_2 over $Pd/ZnO/Al_2O_3$: Catalyst structure dependence of methanol selectivity. *Applied Catalysis A: General* **2016**, *514*, 51 – 59.

(30) Bahruji, H.; Bowker, M.; Jones, W.; Hayward, J.; Esquius, J. R.; Morgan, D. J.; Hutchings, G. J. PdZn catalysts for CO_2 hydrogenation to methanol using chemical vapour impregnation (CVI). *Faraday Discuss.* **2017**, *197*, 309–324.

(31) Friedrich, M.; Ormeci, A.; Grin, J.; Armbrüster, M. PdZn or ZnPd: Charge transfer and Pd-Pd bonding as the driving force for the tetragonal distortion of the cubic crystal structure. *Zeitschrift für anorganische und allgemeine Chemie* **2010**, *636*, 1735.

(32) Tsai, A.; Kameoka, S.; Nozawa, K.; Shimoda, M.; Ishii, Y. Intermetallic: A Pseudoelement for Catalysis. *Acc. Chem. Res.* **2017**, *50*, 2879–2885.

(33) Nozawa, K.; Endo, N.; Kameoka, S.; Tsai, A. P.; Ishii, Y. Catalytic Properties Dominated by Electronic Structures in PdZn, NiZn, and PtZn Intermetallic Compounds. *J. Phys. Soc. Jpn.* **2011**, *80*, 064801.

(34) Krajci, M.; Tsai, A.-P.; Hafner, J. Understanding the Selectivity of Methanol Steam Reforming on the (111) Surfaces of NiZn, PdZn and PtZn: Insights from DFT. *J. Catal.* **2015**, *330*, 6–18.

(35) Li, X.; Li, L.; Lin, J.; Qiao, B.; Yang, X.; Wang, A.; Wang, X. Reactivity of Methanol Steam Reforming on ZnPd Intermetallic Catalyst: Understanding from Microcalorimetric and FT-IR Studies. *J. Phys. Chem. C* **2018**, *122*, 12395–12403.

(36) Chen, Z.-X.; Neyman, K. M.; Gordienko, A. B.; Rösch, N. Surface structure and stability of PdZn and PtZn alloys: Density-functional slab model studies. *Phys. Rev. B* **2003**, *68*, 075417.

(37) Tran, R.; Xu, Z.; Radhakrishnan, B.; Winston, D.; Sun, W.; Persson, K.; Ping-Ong, S. Surface Energies of Elemental Crystals. *Scientific Data* **2016**, *3*, 160080.

(38) Bayer, A.; Flechtner, K.; Denecke, R.; Steinruck, H.; Neyman, K.; Rosch, N. Electronic properties of thin Zn layers on Pd(111) during growth and alloying. *Surface Science* **2006**, *600*, 78–94.

(39) Chen, Z.-X.; Neyman, K.; Rösch, N. Theoretical study of segregation of Zn and Pd in Pd-In alloys. *Surface Science* **2004**, *548*, 291–300.

(40) Mills, G.; Jonsson, H.; Schenter, G. K. Reversible work transition state theory: application to dissociative adsorption of hydrogen. *Surface Science* **1995**, *324*, 305.

(41) Jónsson, H.; Mills, G.; Jacobsen, K. W. *Classical and Quantum Dynamics in Condensed Phase Simulations*, b. j. berne and g. ciccotti and d. f. coker ed.; World Scientific: New-York, 1998; Chapter Nudged elastic band method for finding minimum energy paths of transitions (chapter 16), p 385.

(42) Henkelman, G.; Uberuaga, B. P.; Jónsson, H. A climbing image nudged elastic band method for finding saddle points and minimum energy paths. *J. Chem. Phys.* **2000**, *113*, 9901.

(43) Henkelman, G.; ; Jónsson, H. Improved tangent estimate in the nudged elastic band method for finding minimum energy paths and saddle points. *J. Chem. Phys.* **2000**, *113*, 9978.

(44) Podrojkova, N.; Sans, V.; Orinak, A.; Orinakova, R. Recent Developments in the Modelling of Heterogeneous Catalysts for CO_2 Conversion to Chemicals. *ChemCatChem* **2020**, *12*, 1802–1825.

(45) Burghaus, U. Surface chemistry of CO_2 – Adsorption of carbon dioxide on clean surfaces at ultrahigh vacuum. *Prog. Surf. Sci.* **2014**, *89*, 161–217.

(46) Hu, J.; Guo, W.; Liu, Z.-H.; Lu, X.; Zhu, H.; Shi, F.; Yan, J.; ; Jiang, R. Unraveling the Mechanism of the Zn-Improved Catalytic Activity of Pd-Based Catalysts for Water Gas Shift Reaction. *J. Phys. Chem. C* **2016**, *120*, 20181–20191.

(47) Chelli, R.; Pagliai, M.; Procacci, P.; Cardini, G.; Schettino, V. Polarization response of water and methanol investigated by a polarizable force field and density functional theory calculations: Implications for charge transfer. *J. Chem. Phys.* **2005**, *122*, 074504.

(48) Zhong, J.; Yang, X.; Wu, Z.; Liang, B.; Huang, Y.; Zhang, T. State of the art and perspectives in heterogeneous catalysis of CO2 hydrogenation to methanol. *Chem. Soc. Rev.* **2020**, *49*, 1385–1413.

(49) Rasmussen, P.; Holmblad, P.; Askgaar, T.; Ovesen, C.; Stoltze, P.; Norskov, J.; Chorkendorff, I. Methanol synthesis on Cu(100) from a binary gas mixture of CO_2 and H_2. *Catal. Lett.* **1994**, *26*, 373–381.

(50) Rasmussen, P.; Kazuta, M.; Chorkendorff, I. Synthesis of methanol from a mixture of H_2 and CO_2 on Cu(100). *Surface Science* **1994**, *318*, 267 – 280.

(51) Yang, Y.; Evans, J.; Rodriguez, J. A.; White, M. G.; Liu, P. Fundamental studies of methanol synthesis from CO_2 hydrogenation on Cu(111), Cu clusters, and Cu/ZnO(0001). *Phys. Chem. Chem. Phys.* **2010**, *12*, 9909–9917.

(52) Grabow, L. C.; Mavrikakis, M. Mechanism of Methanol Synthesis on Cu through CO_2 and CO Hydrogenation. *ACS Catal.* **2011**, *1*, 365–384.

(53) Fisher, I. A.; Bell, A. T. In-Situ Infrared Study of Methanol Synthesis from H_2/CO_2 over Cu/SiO_2 and $Cu/ZrO_2/SiO_2$. *J. Catal.* **1997**, *172*, 222 – 237.

(54) Hong, Q.-J.; Liu, Z.-P. Mechanism of CO_2 hydrogenation over Cu/ZrO_2(-212) interface from first-principles kinetics Monte Carlo simulations. *Surface Science* **2010**, *604*, 1869 – 1876.

(55) Behrens, M.; Studt, F.; Kasatkin, I.; Kühl, S.; Hävecker, M.; Abild-Pedersen, F.; Zander, S.; Girgsdies, F.; Kurr, P.; Kniep, B.-L. et al. The Active Site of Methanol Synthesis over $Cu/ZnO/Al_2O_3$ Industrial Catalysts. *Science* **2012**, *336*, 893–897.

(56) Kunkes, E. L.; Studt, F.; Abild-Pedersen, F.; Schlögl, R.; Behrens, M. Hydrogenation of CO_2 to methanol and CO on $Cu/ZnO/Al_2O_3$: Is there a common intermediate or not? *J. Catal.* **2015**, *328*, 43 – 48.

(57) Wang, Y.; Kattel, S.; Gao, W.; Li, K.; Liu, P.; Chen, J. G.; Wang, H. Exploring the ternary interactions in Cu–ZnO–ZrO_2 catalysts for efficient CO_2 hydrogenation to methanol. *Nat. Comm.* **2019**, *10*, 1166.

(58) Posada-Perez, S.; Ramirez, P.; Gutierrez, R.; Stacchiola, D.; Vines, F.; Liu, P.; Illas, F.; Rodriguez, J. A. The conversion of CO_2 to methanol on orthorhombic β-Mo_2C and Cu/β-Mo_2C catalysts: mechanism for admetal induced change in the selectivity and activity. *Catal. Sci. Technol.* **2016**, *6*, 6766–6777.

(59) Fujitani, T.; Nakamura, I.; Uchijima, T.; Nakamura, J. The kinetics and mechanism of methanol synthesis by hydrogenation of CO_2 over a Zn-deposited Cu(111) surface. *Surface Science* **1997**, *383*, 285 – 298.

(60) Nakamura, I.; Fujitani, T.; Uchijima, T.; Nakamura, J. The synthesis of methanol and the reverse water-gas shift reaction over Zn-deposited Cu(100) and Cu(110) surfaces: comparison with Zn/Cu(111). *Surface Science* **1998**, *400*, 387 – 400.

(61) Shi, Z.; Tan, Q.; Tian, C.; Pan, Y.; Sun, X.; Zhang, J.; Wu, D. CO_2 hydrogenation to methanol over Cu-In intermetallic catalysts: Effect of reduction temperature. *J. Catal.* **2019**, *379*, 78 – 89.

(62) Collins, S. E.; Baltanas, M. A.; Bonivardi, A. L. An infrared study of the intermediates of methanol synthesis from carbon dioxide over Pd/β-Ga_2O_3. *J. Catal.* **2004**, *226*, 410 – 421.

(63) Ye, J.; Liu, C.-J.; Mei, D.; Ge, Q. Methanol synthesis from CO_2 hydrogenation over a Pd_4/In_2O_3 model catalyst: A combined DFT and kinetic study. *J. Catal.* **2014**, *317*, 44 – 53.

(64) Yang, Y.; White, M. G.; Liu, P. Theoretical Study of Methanol Synthesis from CO_2 Hydrogenation on Metal-Doped Cu(111) Surfaces. *J. Phys. Chem. C* **2012**, *116*, 248–256.

(65) Jiang, X.; Koizumi, N.; Guo, X.; Song, C. Bimetallic Pd–Cu catalysts for selective CO_2 hydrogenation to methanol. *Applied Catalysis B: Environmental* **2015**, *170-171*, 173 – 185.

(66) Borasio, M.; de la Fuente, O. R.; Rupprechter, G.; Freund, H.-J. In Situ Studies of Methanol Decomposition and Oxidation on Pd(111) by PM-IRAS and XPS Spectroscopy. *J. Phys. Chem. B* **2005**, *109*, 17791–17794.

(67) Jiang, X.; Nie, X.; Guo, X.; Song, C.; Chen, J. G. Recent Advances in Carbon Dioxide Hydrogenation to Methanol via Heterogeneous Catalysis. *Chemical Reviews*

(68) Tang, Q.; Shen, Z.; Huang, L.; He, T.; Adidharma, H.; Russell, A.; Fan, M. Synthesis of methanol from CO_2 hydrogenation promoted by dissociative adsorption of hydrogen on a Ga_3Ni_5 (221) surface. *Phys. Chem. Chem. Phys.* **2017**, *19*, 18539–18555.

(69) Liu, L.; Yao, H.; Jiang, Z.; Fang, T. Theoretical study of methanol synthesis from CO_2 hydrogenation on $PdCu_3$(111) surface. *Applied Surface Science* **2018**, *451*, 333 – 345.

(70) Zhao, Y.-F.; Yang, Y.; Mims, C.; Peden, C. H.; Li, J.; Mei, D. Insight into methanol synthesis from CO_2 hydrogenation on Cu(111): Complex reaction network and the effects of H_2O. *J. Catal.* **2011**, *281*, 199–211.

(71) Shan, A.; Zaman, S. F.; AlZahrani, A. A.; Daous, M. A.; Driss, H.; Petrov, L. A. Development of Highly Selective PdZn/CeO_2 and Ca-doped PdZn/CeO_2 catalysts for Methanol Synthesis from CO_2 Hydrogenation. *App. Catalysis A.* **2018**, *560*, 42–53.

(72) Wu, P.; Yang, B. Intermetallic PdIn catalyst for CO_2 hydrogenation to methanol: mechanistic studies with a combined DFT and microkinetic modeling method. *Catal. Sci. Technol.* **2019**, *9*, 6102.

(73) Nie, X.; Jiang, X.; Wang, H.; Luo, W.; Janik, M. J.; Chen, Y.; Guo, X.; Song, C. Mechanistic Understanding of Alloy Effect and Water Promotion for Pd-Cu Bimetallic Catalysts in CO_2 Hydrogenation to Methanol. *ACS Catal.* **2018**, *8*, 4873–4892.

(74) Li, S.; Scaranto, J.; Mavrikakis, M. On the Structure Sensitivity of Formic Acid Decomposition on Cu Catalysts. *Top. Catal.* **2016**, *59*, 1580–1588.

(75) Scaranto, J.; Mavrikakis, M. Density functional theory studies of HCOOH decomposition on Pd(111). *Surf. Sci.* **2016**, *650*, 111–120.

(76) Chen, Z.-X.; Neyman, K.; Lim, K.; Rösch, N. CH_3O Decomposition on PdZn(111), Pd(111), and Cu(111). A Theoretical Study. *Langmuir* **2004**, *20*, 8068–8077.

(77) Jeroro, E.; Vohs, J. M. Zn Modification of the Reactivity of Pd(111) Toward Methanol and Formaldehyde. *J. Am. Chem. Soc.* **2008**, *130*, 10199–10207.

(78) Halevi, B.; Peterson, E. J.; Roy, A.; DeLariva, A.; Jeroro, E.; Gao, F.; Wang, Y.; Vohs, J. M.; Kiefer, B.; Kunkes, E. et al. Catalytic Reactivity of Face Centered Cubic $PdZn_\alpha$ for the Steam Reforming of Methanol. *J. Catal.* **2012**, *291*, 44 – 54.

(79) Smith, G. K.; Lin, S.; Lai, W.; Datye, A.; Xie, D.; Guo, H. Initial steps in methanol steam reforming on PdZn and ZnO surfaces: Density functional theory studies. *Surface Science* **2011**, *605*, 750 – 759.

(80) Zhang, M.; Wu, Y.; Dou, M.; Yu, Y. A DFT Study of Methanol Synthesis from CO_2 Hydrogenation on the Pd(111) Surface. *Catalysis letters* **2018**, *148*, 2935–2944.

(81) Ota, A.; Kunkes, E. L.; Kasatkin, I.; Groppo, E.; Ferri, D.; Poceiro, B.; Navarro-Yerga, R. M.; Behrens, M. Comparative study of hydrotalcite-derived supported Pd_2Ga and PdZn intermetallic nanoparticles as methanol synthesis and methanol steam reforming catalysts. *J. Catal.* **2012**, *293*, 27–38.

(82) Kresse, G.; Hafner, J. Ab Initio Molecular Dynamics for Liquid Metals. *Phys. Rev. B* **1993**, *47*, 558–561.

(83) Kresse, G.; Furthmüller, J. Efficient Iterative Schemes for Ab Initio Total-Energy Calculations Using A Plane-Wave Basis Set. *Phys. Rev. B* **1996**, *54*, 11169 – 11186.

(84) Kresse, G.; Furthmüller, J. Efficiency of Ab-Initio Total Energy Calculations For Metals and Semiconductors Using a Plane Wave Basis Set. *Comput. Mater. Sci.* **1996**, *6*, 15–50.

(85) Blochl, P. E. Projector Augmented-Wave Method. *Phys. Rev. B* **1994**, *50*, 17953–17979.

(86) Kresse, G.; Joubert, D. From Ultrasoft Pseudopotentials To the Projector Augmented-Wave Method. *Phys. Rev. B* **1999**, *59*, 1758–1775.

(87) Perdew, J. P.; Burke, K.; Ernzerhof, M. Erratum: Generalized Gradient Approximation Made Simple. *Phys. Rev. Lett.* **1997**, *78*, 1396.

(88) Grimme, S.; Ehrlich, S.; Goerigk, L. Effect of The Damping Function in Dispersion Corrected Density Functional Theory. *J. Comput. Chem.* **2011**, *32*, 1456.

(89) Lin, S.; Xie, D.; Guo, H. Pathways of Methanol Steam Reforming on PdZn and Comparison with Cu. *The Journal of Physical Chemistry C* **2011**, *115*, 20583–20589.

(90) Hansen, M. *Constitution of Binary Alloys, 2nd ed.*; McGraw Hill: New York, 1958.